2014

Serial Cervicovaginal Exposures with Replication-Deficient SIVsm Induce Higher Dendritic Cell (pDC) and CD4+ T-Cell Infiltrates Not Associated with Prevention but a More Severe SIVmac251 Infection of Rhesus Macaques

Shaheed A. Abdulhaqq
Wistar Institute

Melween I. Martinez
University of Puerto Rico, melween.martinez@upr.edu

Guobin Kang
University of Minnesota Medical School, gkang2@unl.edu

Andrea S. Foulkes
University of Massachusetts

Idia V. Rodriguez
University of Puerto Rico (UPR)

See next page for additional authors

Published in *Journal of Acquired Immune Deficiency Syndromes* 65:4 (April 1, 2014), pp. 405–413

Submitted for publication October 25, 2013; accepted October 25, 2013.

Presented at the Nonhuman Primate Models for AIDS 29th Annual Symposium, October 25–28, 2011, Seattle, Washington, USA.
The authors have no conflicts of interest to disclose.

Supplemental content for this article is available following the references.

Serial Cervicovaginal Exposures with Replication-Deficient SIVsm Induce Higher Dendritic Cell (pDC) and CD4+ T-Cell Infiltrates Not Associated with Prevention but a More Severe SIVmac251 Infection of Rhesus Macaques

Shaheed A. Abdulhaqq, BS,[1] Melween I. Martinez, DVM,[2]

Guobin Kang, BS,[3] Andrea S. Foulkes, ScD,[4] Idia V. Rodriguez, DVM,[2]

Stephanie M. Nichols, PhD,[2] Meredith Hunter, MS,[5]

Carlos A. Sariol, MD,[2, 6, 7] Lynnette A. Ruiz, PhD,[2] Brian N. Ross, MS,[1]

Xiangfan Yin, MS,[1] David W. Speicher, PhD,[1] Ashley T. Haase, MD,[3]

Preston A. Marx, PhD,[5] Qingsheng Li, PhD,[8, 9]

Edmundo N. Kraiselburd, PhD,[2] and Luis J. Montaner, DVM, PhD[1]

1. Department of Immunology, The Wistar Institute, Philadelphia, Pennsylvania USA
2. Caribbean Primate Research Center and Animal Resources Center, University of Puerto Rico (UPR), San Juan, Puerto Rico
3. University of Minnesota Medical School, Minneapolis, Minnesota, USA
4. Division of Biostatistics and Epidemiology, University of Massachusetts, Amherst, Massachusetts, USA
5. Tulane National Primate Research Center, Covington, Louisiana, USA
6. Department of Microbiology, UPR Medical School, San Juan, Puerto Rico
7. Department of Internal Medicine, UPR Medical School, San Juan, Puerto Rico
8. School of Biological Sciences, University of Nebraska, Lincoln, Nebraska, USA
9. Nebraska Center for Virology, University of Nebraska, Lincoln, Nebraska, USA

Corresponding author – Luis J. Montaner, DVM, Department of Immunology, The Wistar Institute, 3601 Spruce Street, Philadelphia, PA 19104, email montaner@wistar.org

Abstract

Objective: Intravaginal exposure to simian immunodeficiency virus (SIV) acutely recruits interferon-alpha (IFN-α) producing plasmacytoid dendritic cells (pDC) and CD4$^+$ T-lymphocyte targets to the endocervix of nonhuman primates. We tested the impact of repeated cervicovaginal exposures to noninfectious, defective SIV particles over 72 hours on a subsequent cervicovaginal challenge with replication competent SIV. *Methods:* Thirty-four female Indian Rhesus macaques were given a 3-day twice-daily vaginal exposures to either SIVsmB7, a replication deficient derivative of SIVsmH3 produced by a T lymphoblast CEMx174 cell clone (n = 16), or to CEM supernatant controls (n = 18). On the fourth day, animals were either euthanized to assess cervicovaginal immune cell infiltration or intravaginally challenged with SIVmac251. Challenged animals were tracked for plasma viral load and CD4 counts and euthanized at 42 days after infection. *Results:* At the time of challenge, macaques exposed to SIVsmB7, had higher levels of cervical CD123 pDCs ($P = 0.032$) and CD4$^+$ T cells ($P = 0.036$) than those exposed to CEM control. Vaginal tissues showed a significant increase in CD4$^+$ T-cell infiltrates ($P = 0.048$) and a trend toward increased CD68$^+$ cellular infiltrates. After challenge, 12 SIVsmB7-treated macaques showed 2.5-fold greater daily rate of CD4 decline ($P = 0.0408$), and viral load rise ($P = 0.0036$) as compared with 12 control animals. **Conclusions:** Repeated nonproductive exposure to viral particles within a short daily time frame did not protect against infection despite pDC recruitment, resulting instead in an accelerated CD4$^+$ T-cell loss with an increased rate of viral replication.

Keywords: simian immunodeficiency virus, nonhuman primate, CD4, plasmacytoid dendritic cells, cervicovaginal mucosa

Introduction

Women comprise over half of all individuals living with HIV-1 worldwide with intravaginal sex as the predominant route of transmission.[1] However, the rate of infection among exposed females is statistically low, indicating that only a fraction of viral exposures result in productive infection.[2–5] At each exposure, HIV can interact with the cervical epithelium[6,7] mediating cellular infiltration[6,8] and potentially engaging Toll-like receptor (TLR) 7 on dendritic cells.[8–10] The effects of nonproductive HIV-1 or simian immunodeficiency virus (SIV)

cervicovaginal exposures (absent infection) on subsequent infection outcomes remain unclear.

The CAPRISA004 trial found a positive association between a preexisting inflammatory cytokine profile within cervicovaginal fluids and subsequent HIV infection,[11] supporting previously held views that vaginal immune activation increases HIV-1 infectivity. In parallel, a study examining SIV infectivity in rhesus macaques after direct topical application of TLR-7/9 ligands to the cervicovaginal mucosa showed increased localized inflammation and increased viral load after challenge.[12] However, there are well-documented cases of women with a history of chronic multiyear HIV-1 exposure without infection indicating that exposure-initiated mechanisms may reduce future infectivity on reexposure.[13–15] Of interest, studies of resistance in these women have largely failed to identify HIV-specific responses as a determinant of protection[15] but a loss of HIV-1 "resistance" in a subset of these women after reduced sex work (i.e., HIV-1 exposure) has suggested that resistance is sustained by innate rather than adaptive responses.[16]

Acute cellular changes after cervicovaginal mucosal infection have been studied. Infection is established within $CD4^+$ T cells and other permissive cells of the lamina propria[17–20] following a robust cellular infiltrate of plasmacytoid dendritic cells (pDCs) and CD4 T cells,[6] and increased mRNA expression of proinflammatory cytokines/chemokines by day 3 post infection (DPI).[21] Of interest, Li et al. demonstrated that infiltrating cervical pDCs produce interferon-alpha (IFN-α) within hours of SIV exposure, preceding $CD4^+$ T-cell infiltrates by 72 hours.[6]

The anti-HIV properties of pDCs and type I IFN have been documented and involve intrinsic and secondary antiviral mechanisms, such as the induction of tetherin or APOPBEC family members, and the modulation of innate and adaptive effectors.[22–27] In a recent clinical study in individuals with chronic HIV infection, IFN immunotherapy sustained viral suppression during antiretroviral therapy interruption in a subset of subjects supporting the interpretation that IFN can inhibit HIV-1 production/replication.[28] However, the role of infiltrating pDCs as a source of type I IFNs and its impact on acute SIV infection if present before infection as a result of repeated noninfectious viral exposures remains unclear. Taking advantage of a replication-deficient SIVsmB7 clone derived from SIVsmH3, able to bind CD4 and fuse with its target without subsequent viral replication,[29–31] we tested the hypothesis that repeated vaginal exposures to SIV in the absence of productive infection would decrease viral infection potential and/or decrease replication kinetics as a consequence of sustained cervical pDC infiltration despite the increase in local $CD4^+$ T-cell infiltrates.

Methods

Ethics Statement and Animal Procedures

Healthy Indian Rhesus monkeys (*Macaca mulata*) were acquired from the Caribbean Primate Research Center of the University of Puerto Rico (UPR)—Medical Sciences Campus (MSC). Animals were quarantined for 6 months and maintained at the AAALAC-accredited facilities of the Animal Resources Center, UPR-MSC.

All animal studies were approved by the UPR-MSC, Institutional Animal Care and Use Committee (IACUC), and comply with the Guide for the Care and Use of Laboratory Animals. Animal Welfare Assurance number: A3421, Protocol number: 3380308.

In addition, steps were taken to reduce suffering in accordance with the recommendations of the Weatherall report, "The Use of Nonhuman Primates in Research." For instance, all procedures were conducted under anesthesia by using ketamine 10–20 mg/kg, delivered intramuscular.

Phase I: 10 (6 and 4) macaques were given either intravaginal SIVsmB7 or CEM mock control inoculations. Inoculations were given twice daily for 3 days in either the follicular or luteal phase, as shown in figure 1 and figure S1 (see the supplemental content following the references). Macaques were euthanized on the fourth day.

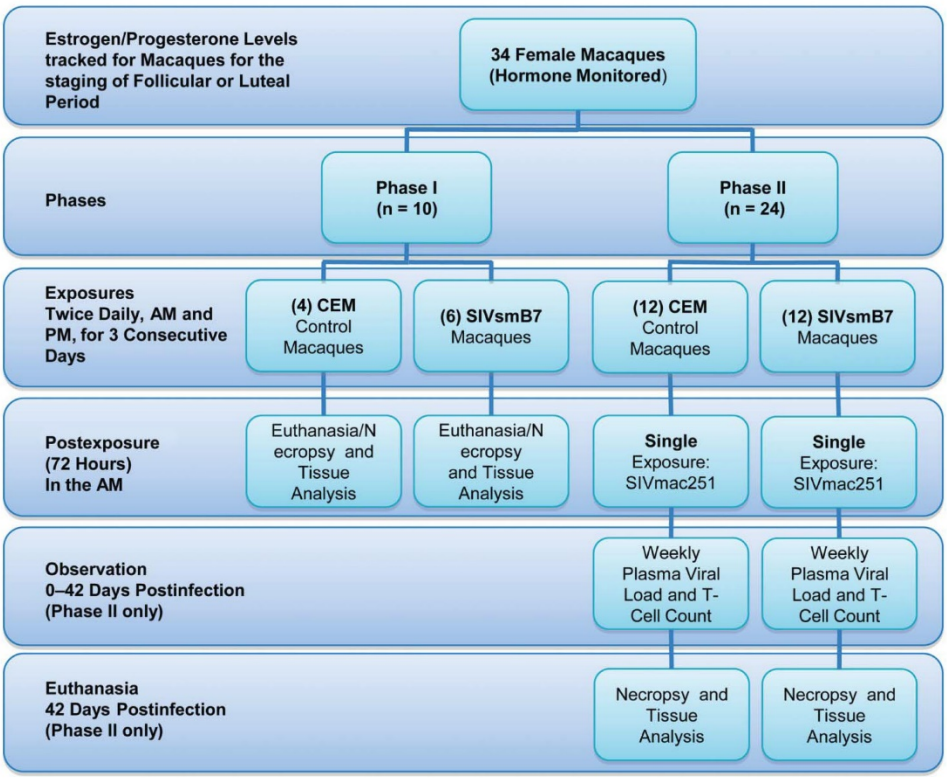

Figure 1. Phase I/II criteria. The study was separated into 2 separate phases. Ten macaques were used in phase I: 4 CEM mock control intravaginally inoculated animals and 6 SIVsmB7 intravaginally inoculated animals. These animals were used to assess cellular infiltration in the cervical and vaginal epithelium. For phase II, 24 animals were divided equally either into CEM mock control– or SIVsmB7-inoculated animals. The inoculation sequence for phase I was repeated and SIVmac251 challenge.

Phase II: Female macaques were housed together before use in the study to allow the animals to reach menstrual synchrony. Twenty-four macaques, 12 macaques per group,

were given either intravaginal SIVsmB7 or CEM mock control inoculations (table 1 and fig. 1). Inoculations were given twice daily for 3 days during the luteal phase. On the fourth day after inoculation, each macaque was given a single 1 mL challenge dose SIVmac251. Blood was taken before the challenge and on days 7, 14, 21, and 42 to determine plasma viral load and CD4 count. Macaques were euthanized on days[42–46] based on the analysis focused on early viral kinetics after a single exposure and infection.

Table 1. Baseline Parameters at the Time of Challenge for Phase II Animals

	CEM Mock Control Treated (12 Macaques)	SIVsmB7 Treated (12 Macaques)	*P*[a]
Age (yrs)	5.0 (4–10)	4.0 (3–6)	0.0249
Weight (kg)	5.43 (3.86–11.05)	5.11 (4.26–6.24)	0.2603
Day of challenge[b]	41.58 (25–62)	38.50 (24–62)	0.8172
CD4 count (cells/mL)	733.0 (449.0–1085)	768.0 (602.0–1379)	0.1749
CD8 count (cells/mL)	397.5 (218.0–800)	380.0 (198.0–799.0)	0.8174
Estrogen (pg/mL)[c]	80.5 (37.50–149.0)	75.85 (20.0–309.0)	0.8399
Progesterone (ng/mL)[c]	4.75 (1.03–8.44)	3.855 (0.97–8.19)	0.9540
Estrogen: progesterone (ratio)	21.94 (7.603–49.19)	20.82 (7.12–55.16)	0.8399

Median values shown (interquartile range).

a. *P* values assessed using Wilcoxon rank-sum tests.

b. Calculated from time after January 1, 2011 to signify equal timing from the start of the study year.

c. Measured at day of challenge.

Euthanasia was performed only on fully anesthetized animals by injection of pentobarbital sodium at 390 mg/mL; 1 cc/10 lbs IV. Vaginal and cervical tissues were taken for analysis.

Viruses

SIVmac251 was diluted 1:2 from a 20,000 $TCID_{50}$ per milliliter viral stock grown in specific pathogen free rhesus macaque peripheral blood mononuclear cell produced by Dr. Ron Desrosiers (New England National Primate Research Center, Harvard Medical School) and kindly provided by Dr. Nancy Miller (NIAID) through contract #N01-AI-30018. Animals were challenged with 1 mL of the diluted viral stock. In vivo, titration was performed as described in the Supplemental Methods.

SIVsmB7 is a virus-like particle derived from a clone of a CEMx174 cell line stably infected with SIVsmH3. SIVsmB7 is noninfectious because of a 1.6 kbp deletion, including integrase, *vif*, *vpr*, and *vpx* genes. Cell-free SIVsmB7 and CEMx174 supernatant (CEM mock control) were isolated by standard 20% (wt/vol) sucrose gradient ultracentrifugation. P27 enzyme-linked immunosorbent assay was used to determine 500 μg P27 SIVsmB7 dose. CEMx174 dose was established by equal protein quantification with SIVsmB7 dose.

CD4 and CD8 Counts

CD4 and CD8 counts were monitored by TruCount Absolute Count Kits (BD Bioscience, San Jose, California) used according to manufacture protocol.

SIV Viral Loads

Plasma viral load was assessed by quantitative reverse transcriptase-polymerase chain reaction as previously described.[32] Full method can be found in the Supplemental Methods.

Immunohistochemistry

Samples from the vagina and cervix were harvested postmortem from each animal and fixed in 4% paraformaldehyde and embedded in paraffin for sectioning, SafeFix II (Fisher Scientific, Pittsburgh, PA), or frozen. Immunohistochemical staining for CD123, CD68, CD4, and Mx1 was conducted as previously reported6 (For complete method, see Supplemental Methods, http://links.lww.com/QAI/A482). $CD123^+$ cells were considered pDC as a previous report by Li et al6 has shown that $CD123^+$ cells infiltrating into the endocervical subepithelium 3 days after SIV exposure stain positive for both HLA-DR and IFN-α confirming these cells are pDC.

Statistical Analysis

Cross-sectional phase 1 and phase 2 two group comparisons between SIVsmB7-exposed and CEM mock control–inoculated animals were made using Wilcoxon rank-sum tests, Fisher test or Student *t* tests. Two-tailed *P* values less than 0.05 were considered statistically significant.

To evaluate the rate of change for LogVL and CD4, a change-point model with random intercept terms for each monkey and fixed effects for baseline CD4, days-postinfection (DPI) (overall and after 14 DPI), a group indicator for SIVsmB7 exposure, and 2-way interaction terms between DPI and group, was fitted. This model accounts for the within individual correlation in repeated measurements and allows for a different slope before and after 14 DPI. The models are listed below, with model variables estimates described in the results. The function $(\text{DPI}-14)^+ = 0$ when $\text{DPI} \le 14$ and $(\text{DPI}-14)^+ = \text{DPI}-14$ when $\text{DPI} > 14$.

Model Equations for SIVsmB7 or CEM-Inoculated Animals

$$\begin{aligned}\widehat{\text{LogVL}}_{\text{CEM}}/\widehat{\text{CD4}}_{\text{CEM}} = {} & \beta_0 + (\beta_1 \times \text{age}) \\ & + (\beta_2 \times \text{Baseline\_CD4}) \\ & + (\beta_3 \times \text{DPI}) \\ & + (\beta_4 \times (\text{DPI} - 14)^+)\end{aligned}$$

$$\begin{aligned}\widehat{\text{LogVL}}_{\text{SIVsmB7}}/\widehat{\text{CD4}}_{\text{SIVsmB7}} = {} & \left(\beta_0 + \beta_0'\right) + (\beta_1 \times \text{age}) \\ & + (\beta_2 \times \text{Baseline\_CD4}) \\ & + \left(\beta_3 + \beta_3'\right) \times \text{DPI} \\ & + \left(\left(\beta_4 + \beta_4'\right)\right. \\ & \left. \times (\text{DPI} - 14)^+\right).\end{aligned}$$

Statistical analysis was performed using R 2.14.1 and Prism.

Results

Phase I: Acute Cellular Infiltrates after 72 Hours of SIVsmB7/CEM Mock Control Exposure

Ten female macaques followed during their natural luteal or follicular phases were used to initiate 3-day twice-daily SIVsmB7/CEM mock control dosing within a 3-day period after the start of a menstrual phase (as exemplified for 2 luteal-staged animals in fig. S1 in the supplemental content). Animals were inoculated with CEM mock or SIVsmB7 as described in figure 1 and in the methods.

Consistent with previously published data showing that infectious SIV exposure resulted in acute endocervical pDC and $CD4^+$ T-cell infiltration within 3 days of SIV exposure/infection,[6] replication-deficient SIVsmB7-treated animals had a significant higher number of endocervical $CD123^+$ pDC ($P = 0.0317$, mean: 1328 cells/mm^2 vs. 435 cells/mm^2) and CD4 T cells ($P = 0.0357$, CD4 mean: 141.2 cells/mm^2 vs. 17.92 cells/mm^2) as compared with CEM mock control–inoculated animals at 72 hours (fig. 2A) irrespective of hormonal phase. Moreover, in animals exposed to SIVsmB7, we detected a trend in increased expression of Mx1 (an IFN-stimulated gene; fig. 2A) localized in areas enriched for $CD123^+$ cells. This is consistent with recruitment of $CD123^+$ pDCs to the endocervix and local production of type I IFNs. Although exposure to SIVsmB7 did not result in increased vaginal pDC infiltration (fig. 2B), it did result in higher levels of $CD4^+$ cells in vaginal tissues (fig. 2B; $P = 0.0476$; mean, 164.8 cells/mm^2 vs. 37.95 cells/mm^2). Similar to pDCs, SIVsmB7-treated animals had higher (although not statistically significant) levels of CD68 macrophages than control animals in the cervix, but not in the vaginal tissue. Altogether, results confirm that exposure to replication-deficient SIV can modulate the tissue microenvironment, allowing us to directly test how these local viral-induced changes (i.e., pDC and CD4 T-cell infiltrates) would impact a challenge with infectious SIVmac251.

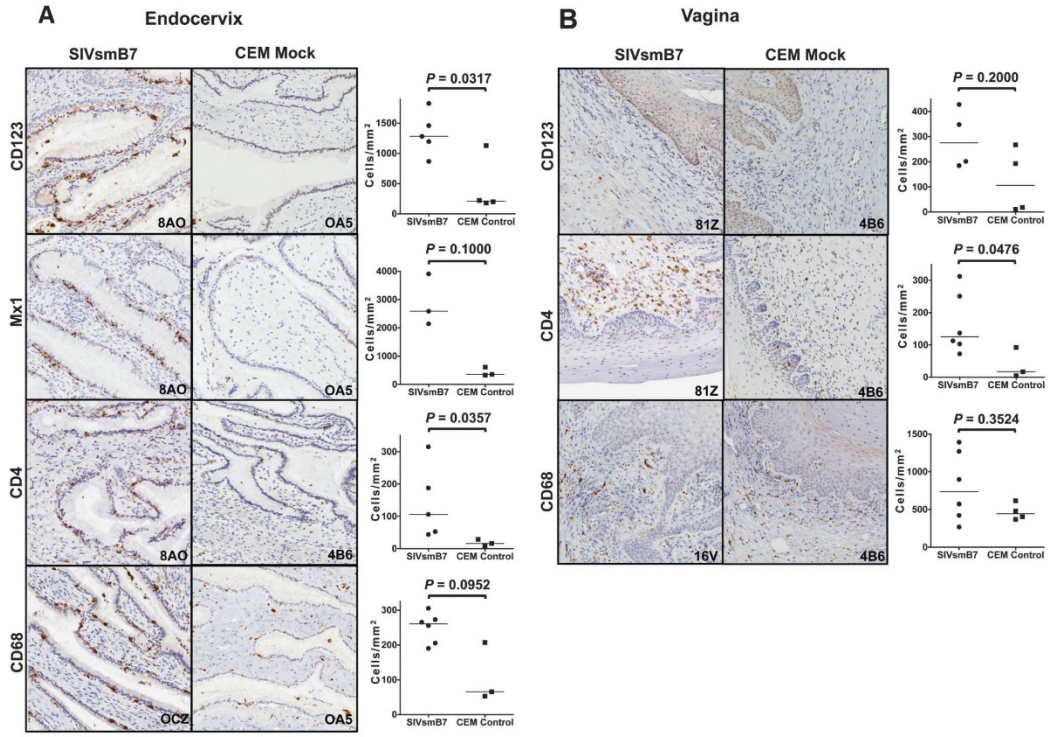

Figure 2. Infiltrate staining and quantification of cervico-vaginal tissue taken from SIVsmB7 and CEM mock control–treated animals. A, Endocervix (top panel: CD123 staining 20×·image); SIVsmB7 treatment (left) induced large-scale pDC infiltration with cells directly underneath or near the columnar epithelium as compared with mock control (P = 0.0317) (second panel: Mx1 staining 20× image); corresponding with increased pDC infiltration in SIVsmB7-treated macaques, there were increased levels of interferon responsive gene product (ISG) Mx1 in treated macaques compared with controls (third panel: CD4 staining 20×·image); SIVsmB7 treatment (left) induced moderate infiltration of $CD4^+$ T cells as compared with CEM mock treatment (P = 0.0357) (bottom panel: CD68 staining 20×·image); SIVsmB7 treatment (left) did not induce a significant increase in macrophage infiltration as compared with CEM mock control (right), but visually, macrophages appeared closer to, and in some cases, permeated the columnar epithelium, suggesting a trend of increased infiltration (P = 0.0952). B, Vagina (top panel: CD123 staining 20× image); SIVsmB7 treatment (left) induced no noticeable level of pDC infiltration as compared with CEM mock control–treated animals (bottom) (P = 0.2000) (middle panel: CD4 staining 20× image); SIVsmB7 treatment (left) induced a sizable increase in CD4 T-cell staining, with many positive staining cells found directly underneath the striated vaginal epithelium and comparably fewer cells found in the vaginal mucosa of CEM mock control–treated animals (right) (P = 0.0476) (bottom panel: CD68 staining 20× image); macaques had moderate levels of macrophage staining within the vaginal mucosa regardless of treatment. This level of CD68 staining was not impacted by treatment (P = 0.3524). Pairwise comparisons were performed with Wilcoxon rank-sum tests.

Phase II: Outcome of SIVmac 251 Infection after 72-Hour Preconditioning with SIVsmB7 or CEM Control

Twenty-four female macaques were challenged with SIVmac251 after undergoing 72-hour exposure (as described above) to either SIVsmB7 (n = 12) or CEM control (n = 12). The groups were similar in weight and inoculation date relative to menstrual cycle (table 1; see fig. S2 in the supplemental content), and there was no significant difference in major histocompatibility complex (MHC) class I allele distribution (Fisher exact test, $P > 0.05$) or for those associated with spontaneous control between groups[33–35] (see table S1 in the supplemental content).

Endogenous estrogen levels at the time of challenge between SIVsmB7 and CEM mock control arms were not significantly different ($P = 0.84$) (table 1), indicating the absence of differences in estrogen-related structural epithelial factors known to impact viral infectivity.[36–38]

As it has been shown that cervicovaginal inflammation is common among captive rhesus macaques,[39] a 28-plex nonhuman primate luminex assay was performed within 1 week of challenge to assess levels of proinflammatory mediators in cervicovaginal lavages (CVL) in 13 of the 24 macaques (6 SIVsmB7/7 CEM mock). Twelve of the cytokines/chemokines tested were below the limit of detection and no cytokine/chemokine tested showed any significant difference between groups. Results for selected cytokines and chemokines are summarized in figure S3 (see supplemental content).

Following a single, intravaginal SIVmac251 challenge using an infectious dose previously determined through an intravaginal titration (see Supplemental Methods), all 24 macaques became infected, with a detectable viral load within 7 or 14 days postinfection (DPI) (fig. 3B). Viral load peaked in all animals by 14–21 DPI, with a mean viral load of 6.63 and 8.02 for CEM mock control– and SIVsmB7-treated, respectively (Student *t* test: $P = 0.0720$).

Although we didn't detect a significant difference in peak viral load, there was a trend toward increased viral load in SIVsmB7-treated macaques as compared with CEM mock–treated animals (fig. 3B). We did detect a statistically significant decline in $CD4^+$ T cells at 14 DPI in SIVsmB7-treated macaques as compared with control animals (Student *t* test: $P = 0.0268$, mean: –355.8 CD4/μl vs. CEM—120.4 CD4/μl) (fig. 3D) consistent with a more severe CD4 depletion after infection in the SIVsmB7-treated females. Notably, 4 of the macaques in the control group (animals 8D4, M847, 31R, and 530) had lower plasma viral loads. These animals were similar to the other animals in the control and experimental groups in terms of MHC genotypes, batch of doses used, day of manipulation, estrogen levels, weight, age, and history of parity (data not shown). Analysis of baseline CVL samples from 2 of these macaques, 53O and 31R, showed no difference to other infected control macaques.

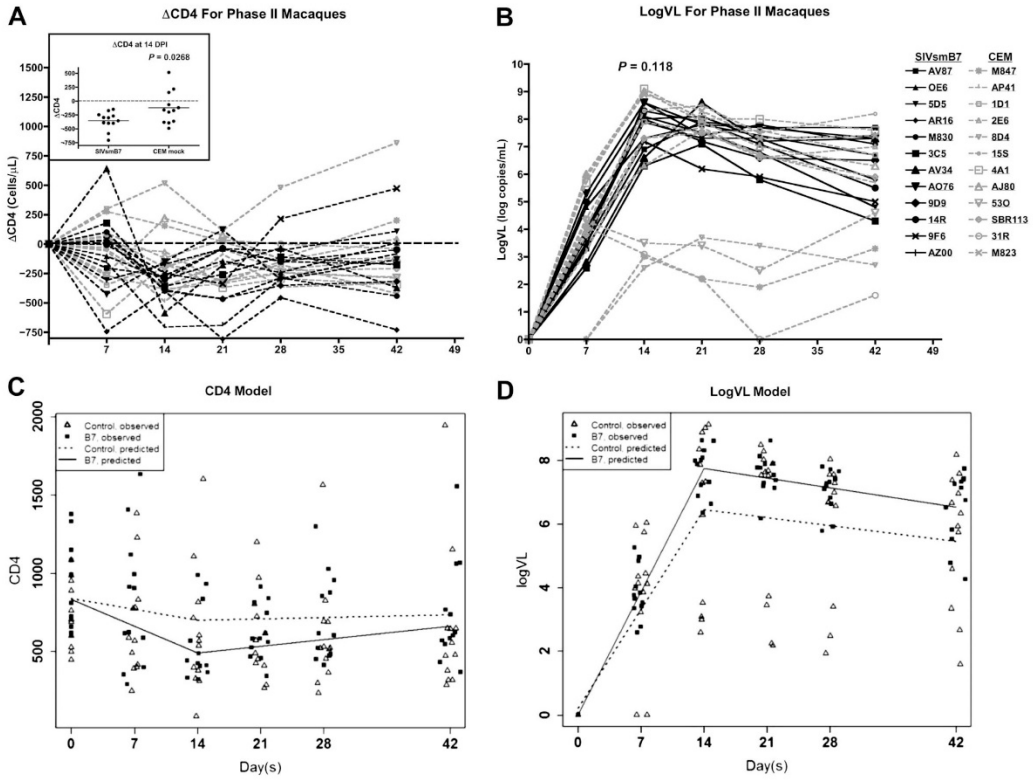

Figure 3. Change-point model of log plasma viral load (LogVL) and CD4 for phase II macaques. A, ΔCD4 for SIVsmB7-treated macaques was significantly higher than in CEM mock control. By 14 DPI, there was mean loss of –355.8 CD4 per microliter in SIVsmB7-treated animals compared with –120.4 CD4 per microliter for controls [Student *t* test; $P = 0.0268$ (inset)]. B, Twenty-two of 24 macaques in both treatment arms reached peak viral load on days 14 or 21. Four of the CEM macaques had significantly lower log viral loads than the remaining 8 CEM mock macaques (*t* test on area under curve with $P < 0.0001$), which was not explained by known correlates of spontaneous SIV control or protection suggesting low viral load was normal variation. At no time point was difference in Log viral load significant; however, starting at 14 DPI and ending at 42 DPI, there was a trend toward increased viremia in SIVsmB7-inoculated macaques (Student *t* test; $P = 0.118$). C, As we detected a significant difference in ΔCD4 between groups, we generated a linear mixed effect spline model to investigate CD4 change between treatment groups over time (in days, as "DPI"). This model predicts an increased loss of $CD4^+$ T cells per day of 14.5 cells per microliter over top of the CEM mock control animals culminating at peak viremia (day 14). D, To investigate the behavior of log viral load, a linear mixed effect spline model for LogVL was also generated. The LogVL model predicts SIVsmB7-treated animals to have an increased log viral load rise per day of 0.106 over top of CEM mock–treated animals up until peak viremia on day 14.

Model of Log Viral Load Rise and CD4 Decline in Phase II Macaques

As our data detected that SIVsmB7 exposures before an infectious challenge caused a significant decline in CD4 at peak viral load after infection, we generated linear models for CD4 or log viral load kinetics over days (DPI) and included a spline (or change-point) at peak viral load day 14 representing the end of the acute change in variables after infection (illustrated in both viral load and CD4 decline data in figs. 3C, D). As expected, both models showed that (1) DPI is a significant determinant of both CD4 decline and viral load rise for animals in either group as exemplified by its coefficient β_3 in control ($P = 0.0436$ for CD4 and $P < 0.0001$ for logVL; Methods and table 2) and β_3' in SIVsmB7 treated ($P = 0.0408$ for CD4 and $P = 0.0036$ for logVL) and (2) day 14 is a valid change-point as illustrated by the reverse of direction of estimates for β_3 and β_4 for the control and β_3' and β_4' for the SIVsmB7 group.

The model for CD4 T-cell kinetics closely approximated our CD4 data and indicated a significantly different change rate between groups before day 14 (β_3', $P = 0.0408$; fig. 3 and table 2). The effect of infection in the CEM mock control animals showed a loss of 10.06 $CD4^+$ T cells per microliter each day until peak viremia (140.8 loss at peak viral load). SIVsmB7-treated macaques had a 2.5-fold higher daily loss of $CD4^+$ T cells totaling 25.0 $CD4^+$ T cells per microliter per day (342.8 loss at peak viral load).

As for viral load, the model showed a significantly higher rate of change in viral load for the SIVsmB7 over CEM control before day 14 (β_3', $P = 0.0036$; fig. 3 and table 2) in support of greater CD4 T-cell loss. Specifically, log viral load rise each day after infection was predicted to be 0.553 log per day in SIVsmB7-treated macaques as compared with 0.446 log per day for CEM mock control animals. Taking into account baseline CD4 count, CD8 count, CD4/CD8 ratio, age, or weight, as independent factors did not change the model's output for viral load rise.

All together, our results suggest that noninfectious SIV exposures and associated conditioning of the local microenvironment result in a greater $CD4^+$ T-cell decline with higher viral load.

Table 2. Intercept and Model Coefficients for CEM Control Versus SIVsmB7-Treated Macaques from Phase II*

Coefficients for LogVL Change-Point Models	Estimate	Standard Error	*P*
β_0	2.340666	1.564118	0.1373
β_1	–0.13222	0.172551	0.4525
β_2	–0.00176	0.001144	0.1396
β_3	0.446266	0.025321	<0.0001*
β_4	–0.48223	0.034106	<0.0001*
β_0'	–0.1968	0.684871	0.7768
β_3'	0.106337	0.035784	0.0036*
β_4'	–0.1141	0.048224	0.0197*
Coefficients for CD4 Change-Point Models	**Estimate**	**Standard Error**	***P***
β_0	323.5255	203.569	0.1147
β_1	–34.6649	22.16708	0.1336
β_2	0.8501	0.14663	<0.0001*
β_3	–10.0638	4.93237	0.0436*
β_4	11.3498	6.64368	0.0903
β_0'	–7.7609	99.82471	0.9388
β_3'	–14.4239	6.97048	0.0408*
β_4'	19.3415	9.39395	0.0418*

*Denotes significant coefficients in the model.

Discussion

We show for the first time that an early, local, innate, and CD4 T-cell response to replication-deficient SIV particles can enhance the rate of $CD4^+$ T-cell decline and viral load rise on a subsequent productive infection. Our results were contrary to our original hypothesis that the observed increase in SIV-induced cervical pDC infiltrates and local IFN-mediated mechanisms would inhibit productive infection. Instead, our data are consistent with viral exposures acutely modulating levels of vaginal and cervical $CD4^+$ T-cell infiltrates, providing a greater preexisting "substrate" for viral infection, potentially overwhelming any inhibition provided by pDC and resulting in an accelerated decrease of $CD4^+$ T cells in association with viral replication. Importantly, our data assessing the impact of recruited pDC were collected during natural progesterone high periods independent of pharmacological treatments commonly used to synchronize animals as these have been shown to impair pDC function.[40,41]

Our results parallel a report by Wang et al. where female macaques were preexposed to TLR-9 or TLR-7 ligands, CpG, or imiquimod, respectively, before and during SIVmac251 challenge.[12] Wang et al. did not quantify differences in cellular infiltrates before challenge nor model viral kinetics to peak viral load, but did observe increased inflammatory cytokines and infiltrate after dosing and a higher viral load 8 weeks after infection. Their reported data are consistent with our observed accelerated CD4 loss and viral load rise in SIVsmB7 pre-exposed animals. We speculate that the Wang et al. study showed a more

marked increase in viral replication than our study due to use to 2 challenges using a SIVmac251 one log higher (greater viral inoculum42) and use of optimized TLR-7/9 ligands, which may have induced a greater inflammatory environment (greater local immune activation[43]).

Importantly, our results are directly relevant to both low-dose SIV repeated challenge study designs commonly used in vaccine studies and to settings of repeated HIV exposures in women. Regarding SIV study designs, our data suggest that early SIV challenges may encounter a different microenvironment than later challenges as a result of immune cell infiltration. Infections after repeated exposures may increase local cell targets and result in accelerated infection kinetics and/or greater gut-associated lymphoid tissue depletion when compared with infections occurring at the start of exposures. Per human cohorts, our data suggest that a sex worker in an area with high HIV-1 prevalence may have different levels of intravaginal immune cell infiltration, independent of coinfections, as compared with women with low levels of HIV-1 exposure. The presence of increased $CD4^+$ T cells and CD68 cells in women at higher risk of HIV-1 infection or in nonhuman primates after multiple SIV exposures may decrease the efficiency of prophylactic interventions by increasing infection efficiency. However, it would be of interest to determine if vaccine-elicited antiviral antibodies in the presence of an increase in cellular infiltration could also provide a greater effector population to harness potentially protective antibody-depended cell-mediated cytotoxicity mechanisms in high-risk uninfected women. Taken together, our data suggest that SIV/HIV exposures can contribute to local immune modulation affecting the host tissue response to future viral infection as already established for other STD coinfections.[4,16,44,45] Future experiments using a lower infectious dose or repeated low to high-dose escalation of virus would be needed to directly show if SIVsmB7 preexposures would increase infection rate over controls as suggested by our data.

Our study had limitations that we addressed. First, our replication-deficient virus, SIVsmB7, was derived from the human cell line, CEMx174. Previous studies have shown that xeno/allogeneic adaptive immune responses to MHC alone can block infection.[46] We found that both SIVsmB7 and CEMx174 supernatants had MHC class I and class II proteins (see fig. S4 in the supplemental content). The 72-hours time frame used for this experiment would limit development of adaptive xenoantigenic responses; moreover, we used a challenge virus derived from a rhesus macaque cell line to avoid this possible confounder response (Methods). It has been shown that innate allogenic responses can be rapid in response to live tissue grafts,[47] yet little is known about the speed and strength of such responses through mucosal administration of MHC proteins. Mucosal studies to date have only examined such responses after the induction of the adaptive response.[48,49] We interpret that because MHC proteins are present in both SIVsmB7 and control, it is unlikely there would be a differential response yet to be detected based on MHC alone. Importantly, $CD4^+$ T-cell and pDC infiltration was significantly greater in SIVsmB7-treated animals indicating the control proteins did not induce change in the absence of SIV proteins. As for other proteins shown in figure S4 and table S2 (see the supplemental content), proteomic analysis of both CEM mock and SIVsmB7 doses had comparable protein content to SIVsmB7 outside the presence of viral proteins or Mov10. Interestingly, the presence of

Mov10 (see table S2 in the supplemental content) in SIVsmB7 proteomic analysis is consistent with enriched particle generation, as previous reports have shown that Mov10 incorporates into viral particles.[50] It has also been shown that ectopic expression of Mov10 is an inhibitor of HIV-1/SIV infectivity[50–53]; however, our data together with a recent report showing that basal levels of Mov10 had no impact on HIV-1 replication or infectivity argues against its antiviral potential.[51]

Second, previous studies have shown that captive rhesus macaques can have divergent preexisting cervicovaginal inflammation.[39,54] To control for this, we did random testing of CVL from rhesus macaques and found no difference in inflammatory cytokine levels between treatment groups (see fig. S3 in the supplemental content) despite observing differential CD4 changes between groups as described. The only difference we did detect was a 1-year difference in age between groups (table 1). We do not expect this minor difference impacts our data as previous research has evidenced no significant difference in immune parameters, such as immune activation or serum cytokine level, among young to middle-age macaques.[55]

Third, our conclusions address the cervicovaginal mucosa and not other mucosal routes of exposure. Future studies will need to establish whether repeated replication-deficient rectal exposures induce $CD4^+$ T-cell infiltration and affect the severity of a productive infection. Intriguingly, sustained SIV-resistance has been reported following repeated low-dose intra-rectal SIV challenges, highlighting a potential difference in compartments or difference between 72 hours versus chronic exposure effects or both.[56]

In conclusion, our data support a model where viral exposures in the absence of productive infection induce changes in cervicovaginal cellular infiltrates that do not prevent infection. Furthermore, our data may indicate an added risk to repeated short-term exposures not previously identified and introduces an unaccounted tissue change variable that may impact the outcome of SIV challenge in studies evaluating protection by low-dose repeated challenge formats using female macaques.

Acknowledgments – The authors acknowledge the critical support received from the UPenn CFAR Viral/Molecular and Nonhuman Primate Core and the TNPRC Flow Cytometry Core Laboratory for immune and viral assays during the study. This study was also made possible by support from the Virology Laboratory, UPR-MSC (T. Arana, P. Pantoja, and R. Medina); the Wistar Institute Cancer Center Proteomics and Histotechnology Core Laboratories (K. Speicher, N. Gorman, T. Beer, and R. Delgiacco). The authors acknowledge additional support from J. Dubin, L. Azzoni, PhD, A. Mackiewicz, and M. Fuller. Supported by NIH Grants R01 AI084142 and R01 AI094603 to E.N.K. and L.J.M., NIH Grant P40 OD012217 to M.I.M., R01 HL107196 to A.S.F., and T32 AI070099 to S.A.A. Additional support was provided by the Philadelphia Foundation (Robert I. Jacobs Fund), Henry S. Miller, Jr. and J. Kenneth Nimblett, AIDS funds from the Commonwealth of Pennsylvania and from the Commonwealth Universal Research Enhancement Program, Pennsylvania Department of Health, the Penn Center for AIDS Research (P30 AI 045008) and Cancer Center Grant (P30 CA10815), the American Foundation for AIDS Research, the National Cancer Institute, National Institutes of Health (Contract No. HHSN261200800001E), and the Intramural Research Program of the NIH, National Cancer Institute, Center for Cancer Research.

References

1. UNAIDS JUNPoHA. *UNAIDS Report on the Global AIDS Epidemic*. Geneva, Switzerland: UNAIDS; 2010.
2. Chakraborty H, Sen PK, Helms RW, et al. Viral burden in genital secretions determines male-to-female sexual transmission of HIV-1: a probabilistic empiric model. *AIDS*. 2001;15:621–627.
3. Gray RH, Wawer MJ. Probability of heterosexual HIV-1 transmission per coital act in sub-Saharan Africa. *J Infect Dis*. 2012;205:351–352.
4. Gray RH, Wawer MJ, Brookmeyer R, et al. Probability of HIV-1 transmission per coital act in monogamous, heterosexual, HIV-1-discordant couples in Rakai, Uganda. *Lancet*. 2001;357:1149–1153.
5. Pilcher CD, Tien HC, Eron JJ Jr, et al. Brief but efficient: acute HIV infection and the sexual transmission of HIV. *J Infect Dis*. 2004;189: 1785–1792.
6. Li Q, Estes JD, Schlievert PM, et al. Glycerol monolaurate prevents mucosal SIV transmission. *Nature*. 2009;458:1034–1038.
7. Miller CJ, Li Q, Abel K, et al. Propagation and dissemination of infection after vaginal transmission of simian immunodeficiency virus. *J Virol*. 2005;79:9217–9227.
8. Megjugorac NJ, Young HA, Amrute SB, et al. Virally stimulated plasmacytoid dendritic cells produce chemokines and induce migration of T and NK cells. *J Leukoc Biol*. 2004;75:504–514.
9. Lepelley A, Louis S, Sourisseau M, et al. Innate sensing of HIV-infected cells. *PLoS Pathog*. 2011;7:e1001284.
10. Zhou D, Kang KH, Spector SA. Production of interferon alpha by human immunodeficiency virus type 1 in human plasmacytoid dendritic cells is dependent on induction of autophagy. *J Infect Dis*. 2012;205:1258–1267.
11. Yonezawa A, Morita R, Takaori-Kondo A, et al. Natural alpha interferon-producing cells respond to human immunodeficiency virus type 1 with alpha interferon production and maturation into dendritic cells. *J Virol*. 2003;77:3777–3784.
12. Wang Y, Abel K, Lantz K, et al. The Toll-like receptor 7 (TLR7) agonist, imiquimod, and the TLR9 agonist, CpG ODN, induce antiviral cytokines and chemokines but do not prevent vaginal transmission of simian immunodeficiency virus when applied intravaginally to rhesus macaques. *J Virol*. 2005;79:14355–14370.
13. Rowland-Jones SL, Dong T, Fowke KR, et al. Cytotoxic T cell responses to multiple conserved HIV epitopes in HIV-resistant prostitutes in Nairobi. *J Clin Invest*. 1998;102:1758–1765.
14. Dorrell L, Hessell AJ, Wang M, et al. Absence of specific mucosal antibody responses in HIV-exposed uninfected sex workers from the Gambia. *AIDS*. 2000;14:1117–1122.
15. Tomescu C, Abdulhaqq S, Montaner LJ. Evidence for the innate immune response as a correlate of protection in human immunodeficiency virus (HIV)-1 highly exposed seronegative subjects (HESN). *Clin Exp Immunol*. 2011;164:158–169.
16. Kaul R, Rowland-Jones SL, Kimani J, et al. Late seroconversion in HIV-resistant Nairobi prostitutes despite preexisting HIV-specific $CD8^+$ responses. *J Clin Invest*. 2001;107:341–349.
17. Gruber A, Norder H, Magnius L, et al. Late seroconversion and high chronicity rate of hepatitis C virus infection in patients with hematologic disorders. *Ann Oncol*. 1993;4:229–234.
18. Oliva JA, Maymo RM, Carrio J, et al. Late seroconversion of C virus markers in hemodialysis patients. *Kidney Int Suppl*. 1993;41:S153–S156.

19. Salazar-Gonzalez JF, Salazar MG, Keele BF, et al. Genetic identity, biological phenotype, and evolutionary pathways of transmitted/founder viruses in acute and early HIV-1 infection. *J Exp Med*. 2009;206:1273–1289.
20. Padilla Navas I, Masia M, Carratala JA, et al. Late seroconversion in Legionella pneumophila pneumonia [in Spanish]. *Rev Clin Esp*. 1993; 192:50–51.
21. Abel K, Rocke DM, Chohan B, et al. Temporal and anatomic relationship between virus replication and cytokine gene expression after vaginal simian immunodeficiency virus infection. *J Virol*. 2005;79:12164–12172.
22. Tomescu C, Chehimi J, Maino VC, et al. NK cell lysis of HIV-1-infected autologous CD4 primary T cells: Requirement for IFN-mediated NK activation by plasmacytoid dendritic cells. *J Immunol*. 2007;179:2097–2104.
23. Aspinall R, Pido-Lopez J, Imami N, et al. Old rhesus macaques treated with interleukin-7 show increased TREC levels and respond well to influenza vaccination. *Rejuvenation Res*. 2007;10:5–17.
24. Peng G, Lei KJ, Jin W, et al. Induction of APOBEC3 family proteins, a defensive maneuver underlying interferon-induced anti-HIV-1 activity. *J Exp Med*. 2006;203:41–46.
25. Chevret S, Costagliola D, Lefrere JJ, et al. A new approach to estimating AIDS incubation times: results in homosexual infected men. *J Epidemiol Community Health*. 1992;46:582–586.
26. Altfeld M, Fadda L, Frleta D, et al. DCs and NK cells: critical effectors in the immune response to HIV-1. *Nat Rev Immunol*. 2011;11:176–186.
27. Hosmalin A, Lebon P. Type I interferon production in HIV-infected patients. *J Leukoc Biol*. 2006;80:984–993.
28. Azzoni L, Foulkes AS, Papasavvas E, et al. Pegylated interferon alfa-2a monotherapy results in suppression of HIV type 1 replication and decreased cell-associated HIV DNA integration. *J Infect Dis*. 2013; 207:213–222.
29. Kraiselburd EN, Torres JV. Properties of virus-like particles produced by SIV-chronically infected human cell clones. *Cell Mol Biol (Noisy-legrand)*. 1995;41(suppl 1):S41–S52.
30. Kraiselburd EN, Salaman A, Beltran M, et al. Vaccine evaluation studies of replication-defective SIVsmB7. *Cell Mol Biol (Noisy-le-grand)*. 1997; 43:915–924.
31. Martinez I, Giavedoni L, Kraiselburd E. Clone B7 cells have a single copy of SIVsmB7 integrated in chromosome 20. *Arch Virol*. 2002;147: 217–223.
32. Mehra S, Golden NA, Dutta NK, et al. Reactivation of latent tuberculosis in rhesus macaques by coinfection with simian immunodeficiency virus. *J Med Primatol*. 2011;40:233–243.
33. Muhl T, Krawczak M, Ten Haaft P, et al. MHC class I alleles influence set-point viral load and survival time in simian immunodeficiency virus-infected rhesus monkeys. *J Immunol*. 2002;169:3438–3446.
34. Loffredo JT, Maxwell J, Qi Y, et al. Mamu-B*08-positive macaques control simian immunodeficiency virus replication. *J Virol*. 2007;81: 8827–8832.
35. Yant LJ, Friedrich TC, Johnson RC, et al. The high-frequency major histocompatibility complex class I allele Mamu-B*17 is associated with control of simian immunodeficiency virus SIVmac239 replication. *J Virol*. 2006;80:5074–5077.
36. Sodora DL, Gettie A, Miller CJ, et al. Vaginal transmission of SIV: assessing infectivity and hormonal influences in macaques inoculated with cell-free and cell-associated viral stocks. *AIDS Res Hum Retroviruses*. 1998;14(suppl 1):S119–S123.

37. Smith SM, Baskin GB, Marx PA. Estrogen protects against vaginal transmission of simian immunodeficiency virus. *J Infect Dis*. 2000;182:708–715.
38. Smith SM, Mefford M, Sodora D, et al. Topical estrogen protects against SIV vaginal transmission without evidence of systemic effect. *AIDS*. 2004;18:1637–1643.
39. Spear G, Rothaeulser K, Fritts L, et al. In captive rhesus macaques, cervicovaginal inflammation is common but not associated with the stable polymicrobial microbiome. *PLoS One*. 2012;7:e52992.
40. Hughes GC, Thomas S, Li C, et al. Cutting edge: progesterone regulates IFN-alpha production by plasmacytoid dendritic cells. *J Immunol*. 2008; 180:2029–2033.
41. Huijbregts RP, Helton ES, Michel KG, et al. Hormonal contraception and HIV-1 infection: medroxyprogesterone acetate suppresses innate and adaptive immune mechanisms. *Endocrinology*. 2013;154:1282–1295.
42. Stone M, Keele BF, Ma ZM, et al. A limited number of simian immunodeficiency virus (SIV) env variants are transmitted to rhesus macaques vaginally inoculated with SIVmac251. *J Virol*. 2010;84:7083–7095.
43. Haaland RE, Hawkins PA, Salazar-Gonzalez J, et al. Inflammatory genital infections mitigate a severe genetic bottleneck in heterosexual transmission of subtype A and C HIV-1. *PLoS Pathog*. 2009;5:e1000274.
44. Terzi R, Niero F, Iemoli E, et al. Late HIV seroconversion after nonoccupational postexposure prophylaxis against HIV with concomitant hepatitis C virus seroconversion. *AIDS*. 2007;21:262–263.
45. Gambel JM, Brown AE, Drabick JJ, et al. Risk of late human immunodeficiency virus type 1 seroconversion in United States soldiers whose initial screening tests were reactive. *Transfusion*. 1995;35:886–887.
46. Shearer G, Boasso A. Alloantigen-based AIDS vaccine: revisiting a "rightfully" discarded promising strategy. *F1000 Med Rep*. 2011;3:12.
47. Liu W, Xiao X, Demirci G, et al. Innate NK cells and macrophages recognize and reject allogeneic nonself in vivo via different mechanisms. *J Immunol*. 2012;188:2703–2711.
48. Bergmeier LA, Babaahmady K, Wang Y, et al. Mucosal alloimmunization elicits T-cell proliferation, CC chemokines, CCR5 antibodies and inhibition of simian immunodeficiency virus infectivity. *J Gen Virol*. 2005;86:2231–2238.
49. Kingsley C, Peters B, Babaahmady K, et al. Heterosexual and homosexual partners practising unprotected sex may develop allogeneic immunity and to a lesser extent tolerance. *PLoS One*. 2009;4:e7938.
50. Wang X, Han Y, Dang Y, et al. Moloney leukemia virus 10 (MOV10) protein inhibits retrovirus replication. *J Biol Chem*. 2010;285:14346–14355.
51. Arjan-Odedra S, Swanson CM, Sherer NM, et al. Endogenous MOV10 inhibits the retrotransposition of endogenous retroelements but not the replication of exogenous retroviruses. *Retrovirology*. 2012;9:53.
52. Burdick R, Smith JL, Chaipan C, et al. P body-associated protein Mov10 inhibits HIV-1 replication at multiple stages. *J Virol*. 2010; 84:10241–10253.
53. Furtak V, Mulky A, Rawlings SA, et al. Perturbation of the P-body component Mov10 inhibits HIV-1 infectivity. *PLoS One*. 2010;5:e9081.
54. Genesca M, Ma ZM, Wang Y, et al. Live-attenuated lentivirus immunization modulates innate immunity and inflammation while protecting rhesus macaques from vaginal simian immunodeficiency virus challenge. *J Virol*. 2012;86:9188–9200.

55. Didier ES, Sugimoto C, Bowers LC, et al. Immune correlates of aging in outdoor-housed captive rhesus macaques (*Macaca mulatta*). *Immun Ageing*. 2012;9:25.
56. Letvin NL, Rao SS, Dang V, et al. No evidence for consistent virus-specific immunity in simian immunodeficiency virus-exposed, uninfected rhesus monkeys. *J Virol*. 2007;81:12368–12374.

Supplemental Digital Content – Methods

SIVsmB7 and CEMx174 Proteomic Analysis

SDS-PAGE Gels
20 μl of B7 and CEM each were loaded to a 12% NuPage 1-mm-thick gel. The gel was stained with Invitrogen Colloidal Coomassie Blue stain.

Protein Digestion
Selected bands were excised from the gel and subsequently destained using 200 μl of 200 mM ammonium bicarbonate and 50% acetonitrile for 30 min with shaking at 37°C and then dried in a SpeedVac. This was followed by reduction/alkylation of the protein band by adding 100 μl 20 mM TCEP in 25 mM ammonium bicarbonate at pH 8.0, incubated for 15 min at 37°C with shaking. The supernatant was discarded and 100 μl of 40 mM iodoacetamide in 25 mM ammonium bicarbonate at pH 8.0 was added and incubated for 30 min at 37°C with shaking. The supernatant was again discarded and two subsequent washes of 200 μl 25 mM ammonium bicarbonate were done for 15 min each with shaking. A final wash was done under the same conditions, except 50% acetonitrile, 25 mM ammonium bicarbonate was used for the wash. The bands were dried in the SpeedVac and were then rehydrated with 20 μl of 0.02 μg/μl modified Trypsin (Promega) in 40 mM ammonium bicarbonate overnight with shaking at 37°C. The next morning, the supernatant was removed to a clean tube on ice and 20 μl of 40 mM ammonium bicarbonate was added to the gel piece for 30 min with shaking at 37°C. The supernatants were combined and 4 μl of neat acetic acid were added to stop the digest.

Protein Identification
4 μls of the combined digest were injected onto a nanocapillary reverse-phase column (self-packed, New Objective 75 um column terminating in a nanospray 15 um tip) directly coupled to a ThermoElectron Orbitrap mass spectrometer. A top six method was used to obtain MS and MS/MS data. A customized database was created using a Simian database with common contaminants and bovine (tagged) added. The database was indexed for partial tryptic searching and the resulting masses and MS/MS spectra from the Orbitrap were searched against this database using the SEQUEST search engine [1, 2]. Subsequent data were filtered using 5 ppm, delta cN of 0.07. Results were reported as spectral counts.

Hormone Measurements
Blood was taken every other day between days 7–23 of the menstrual cycle. Estradiol and progesterone concentrations were measured by enzyme-amplified chemiluminescence (Immulite 1000, Siemens). The analytical limits of sensitivity of the estradiol and progesterone assays were 15 pg/mL (references range of 20–2,000 pg/mL) and 0.1 ng/mL (reference range of 0.2-40 ng/mL), respectively.

Immuno-histochemistry

Tissues were deparaffinized and rehydrated in deionized water. Heat-induced epitope retrieval was performed using the water-bath method (95–98°C for 10–20 min) in 10 mM sodium citrate, pH6.0 for CD123 detection (Sc-681, 1:2000, Santa Cruz Biotechnology Inc.), and Mx1 (1:3000, ProteinTech) and CD68 (KP1, 1:200, Dako). For CD4 detection (IF6, 1:60, Leica Microsystems), epitope retrieval was performed using high-pressure Decloaking Chamber (121°C for 35 sec, Biocare Medical) in 1 mM EDTA, pH 8.0, followed by cooling to room temperature. Tissue sections were blocked with SNIPER Blocking Reagent 5% Non-fat milk (Biocare Medical) for 1 hr at room temperature. Endogenous peroxidase was blocked with 3% (v/v) H2O2 in methanol TBS (pH7.4) 3% [v/v] for CD68, Mx1 and CD123, and 0.9% for CD4 detection). Primary antibodies were diluted in 10% SNIPER Blocking Reagent in TNB blocking buffer (Tris-HCl, pH7.5, 0.15M NaCl, 0.05% Tween 20 with 0.5 Dupont blocking reagent buffer) and incubated overnight at 4°C. After the primary antibody incubation, sections were washed and then incubated with mouse, goat, or rabbit polymer system reagents conjugated with either horseradish peroxidase or alkaline phosphatase (ENVISON kit; Dako) according to the manufacturer's instructions, and developed with 3,3′-diaminobenzidine (Vector Laboratories). Sections were hematoxylin counterstained, mounted in Permount (Fisher Scientific), and examined by light microscopy. Non-specific, IgG was used as isotypic control.

Whole sections of each stained slide were digitized using Scanscope (Aperio), the image was opened in ImageScope, and endocervical areas were selected with ImageScope drawing tools for analysis. CD4+, CD68+, Mx1+ or CD123+ cells were quantified by using a positive pixel count algorithm in the Spectrum Plus analysis program (Version 9.1, Aperio). The parameters of the algorithm were manually tuned to match the specific staining markup image accurately over background DAB stain. Once the parameters were set, the algorithm was applied automatically to all digital slides to measure the number of cells of interest. Data were reported as positive staining cells per square millimeter.

DNA Isolation and MHC Genotyping

Genomic DNA was isolated from a maximum of 3.0 × 106 peripheral blood mononuclear cells using the MagNA Pure LC system (Roche Applied Science) and the MagNA Pure LC DNA Isolation–Large Volume protocol (version 3.0) according to manufacturer's guidelines. The elution volume of extracted DNA was 200 μl of MagNA Pure LC DNA Isolation–Large Volume elution buffer. DNA concentrations (ng/μl) and Abs 260 nm/Abs 280 nm ratios were determined using a NanoDrop UV Spectrophotometer (NanoDrop Technologies). Genotyping for Mamu-A*01, A*02, A*08, A*11, B*01, B* 03, B*04, B*17, B*08, and DRBw*201 was done as previously described [3–5].

Viral Load

Plasma samples were spiked with armored RNA (aRNA; Asurgen) and centrifuged at 25,000 x g for 1 h. Viral RNA (vRNA) was extracted from the pellet with Proteinase K (2.5 μg/μl; Life Tech) and the High Pure Viral RNA kit (Roche). Eluted vRNA (100 μl) was then subjected to the RNA Clean and Concentrator kit (ZYMO Research) and eluted in 50 μl, from which 15 μl were reverse transcribed using MultiScribe™ Reverse Transcriptase (Life

Tech) in a 50-μL gene-specific reaction. Fourteen microliters of cDNA were added to TaqMan gene expression master mix (Life Tech), along with primers and a probe targeting the gag region of SIVmac251, and subjected to 40 cycles of qPCR analyses. Fluorescence signals were detected with an Applied Biosystems 7900HT Sequence Detector. Data were captured and analyzed with Sequence Detector Software (Life Tech). Viral copy numbers were calculated by plotting CT values obtained from samples against a standard curve generated with in vitro-transcribed RNA representing known viral copy numbers. The limit of detection of the assay was five copies per reaction volume or 40 copies per ml of plasma.

SIVmac251 Titration

Infectious challenge was carried out with SIVmac251. The infectious dose via intravaginal delivery was independently determined in a titration study on 15 female rhesus macaques upon vaginal challenge preceding our study. Macaques were intravaginally inoculated with either a single dose of undiluted virus or a 1:5 or 1:10 dilution. All macaques given undiluted virus became infected. Thirty-eight percent of macaques given a 1:5 dilution became infected. To achieve a dose to infect all control animals a 1:2 dilution was chosen for the challenge dose.

References

1. Chittum HS, Lane WS, Carlson BA, Roller PP, Lung FD, Lee BJ, et al. Rabbit beta-globin is extended beyond its UGA stop codon by multiple suppressions and translational reading gaps. *Biochemistry* 1998,37:10866-10870.
2. Yates JR, 3rd, Eng JK, McCormack AL, Schieltz D. Method to correlate tandem mass spectra of modified peptides to amino acid sequences in the protein database. *Analytical Chemistry* 1995,67:1426-1436.
3. Loffredo JT, Maxwell J, Qi Y, Glidden CE, Borchardt GJ, Soma T, et al. Mamu-B*08-positive macaques control simian immunodeficiency virus replication. *Journal of Virology* 2007,81:8827-8832.
4. Kaizu M, Borchardt GJ, Glidden CE, Fisk DL, Loffredo JT, Watkins DI, et al. Molecular typing of major histocompatibility complex class I alleles in the Indian rhesus macaque which restrict SIV CD8+ T cell epitopes. *Immunogenetics* 2007,59:693-703.
5. Kuroda MJ, Schmitz JE, Lekutis C, Nickerson CE, Lifton MA, Franchini G, et al. Human immunodeficiency virus type 1 envelope epitope-specific CD4(+) T lymphocytes in simian/human immunodeficiency virus-infected and vaccinated rhesus monkeys detected using a peptide-major histocompatibility complex class II tetramer. *Journal of Virology* 2000,74:8751-8756.

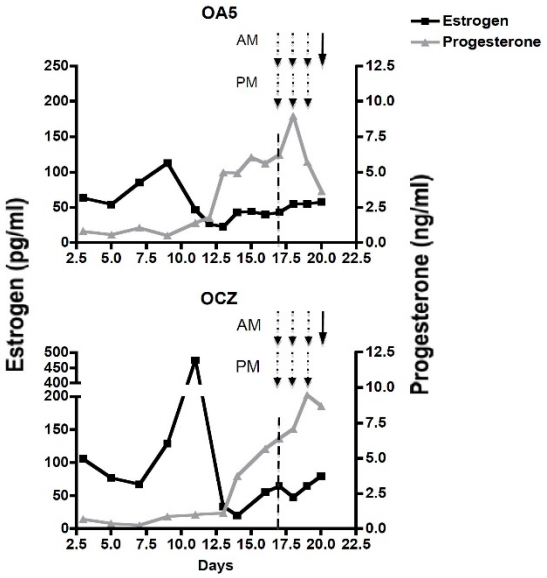

Figure S1. Phase I hormone profiles for luteal phase inoculated macaques. [*Top*] OA5 was inoculated with CEM mock control, and [Bottom] OCZ was inoculated with SIVsmB7. Animal menstrual cycling was tracked for at least one month prior to inoculations to map out hormone profiles (data not shown). Dashed lines indicate start of twice daily, a.m. and p.m., inoculations. Dashed arrows represent individual inoculations as described in Methods. Inoculations were confirmed to take place approximately three days after the start of the luteal phase. Animals were euthanized (solid black arrow) and cervicovaginal tissue sections taken after the final estrogen/progesterone sample was measured. Axis scales were altered to highlight inflection of hormone profiles from follicular to luteal phases. Estrogen (Black Line/Left Axis) Progesterone (Grey Line/Right Axis).

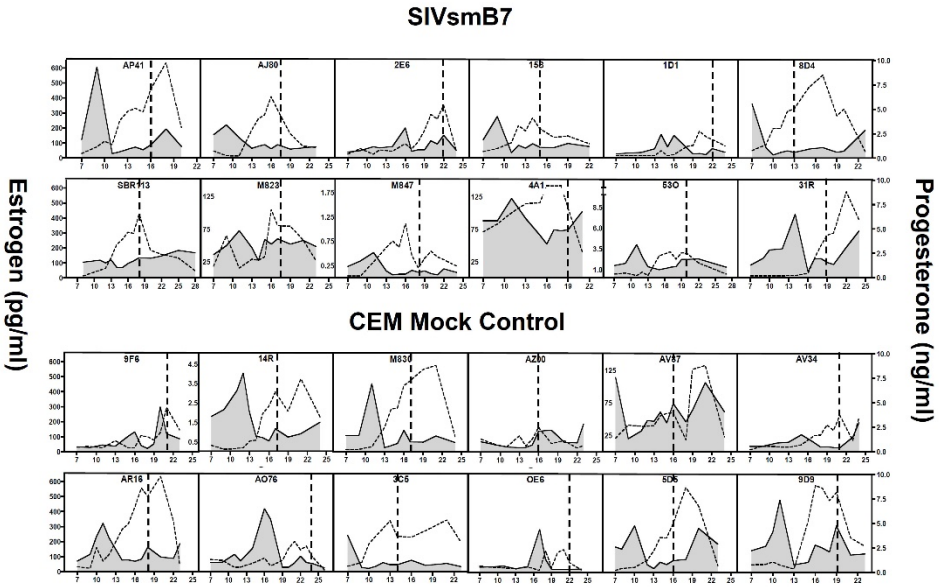

Figure S2. Estrogen/progesterone profiles for Phase II macaques. Estrogen (Grey/Left Axis) Progesterone (Dashed line/Right Axis). Horizontal dashed line indicates SIVmac251 challenge as described in Methods. Macaques were targeted for challenge during the estrogen low, progesterone high luteal phase to avoid potential reduced SIV infectivity during the follicular phase. Axes for M823, 4A1, 9F6, Av87 were modified to show change of menstrual stage.

Table S1. Target MHC I Genotypes for All Phase II Macaques*

Macaque ID	Study Arm	MHC I**
14R	SIVsmB7	A01/B17
3C5	SIVsmB7	A08
5D5	SIVsmB7	A01/A02
9D9	SIVsmB7	—
9F6	SIVsmB7	A01
AO76	SIVsmB7	—
AR16	SIVsmB7	A01
AV34	SIVsmB7	B01
AV87	SIVsmB7	—
AZ00	SIVsmB7	—
M830	SIVsmB7	A02
OE6	SIVsmB7	—
15S	CEM Mock Control	15S
1D1	CEM Mock Control	A08/B01
2E6	CEM Mock Control	A08
31R	CEM Mock Control	—
4A1	CEM Mock Control	A08
53O	CEM Mock Control	A08
8D4	CEM Mock Control	B01
AJ80	CEM Mock Control	A08
AP41	CEM Mock Control	A01
M823	CEM Mock Control	A01
M847	CEM Mock Control	A08
SBR113	CEM Mock Control	A08/B17

* MHC I alleles tested for include A*01, A*02, A*08, A*11, B*01, B* 03, B*04, B*17, and B*08. A*01, B*08 and B*17 have been associated with control of SIV infection in Rhesus macaques [33–35].

** Dashes indicate that macaque had a genotype not assessed within our panel.

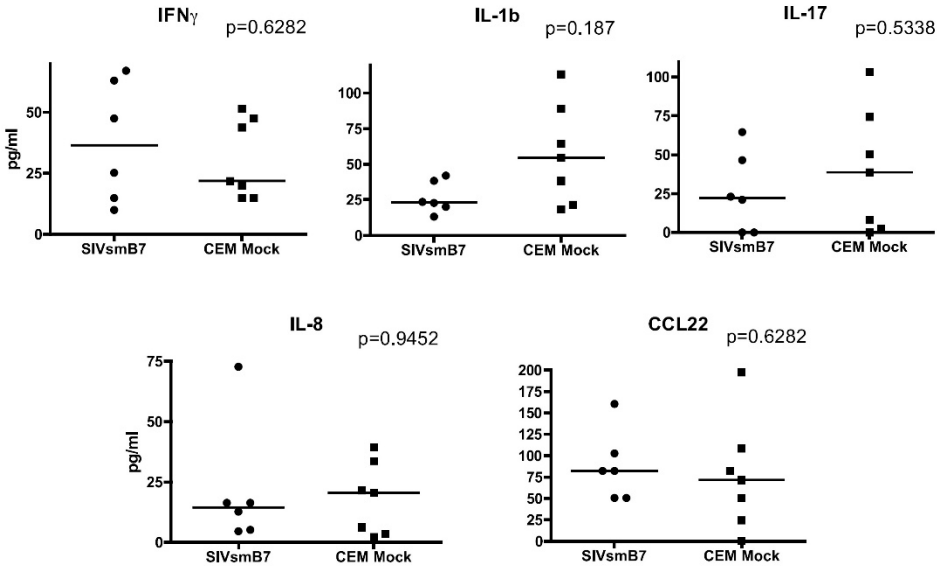

Figure S3. Results from selected cytokines tested in CVL Cytokine Multiplex Assay. Luminex 28-plex Assay (Invitrogen) was done according to manufacturer protocol on PBS lavage samples obtained within 1 week prior to macaque manipulation. Nearly half of the inflammatory cytokines tested were below the level of detection. Of those with detectable levels of cytokine there was no significant differences between macaques, including inflammatory mediators IL-1b, IFNγ, and IL-17 and chemokines IL-8 and CCL22. P-values were generated by two-sided Wilcoxon rank sum tests.

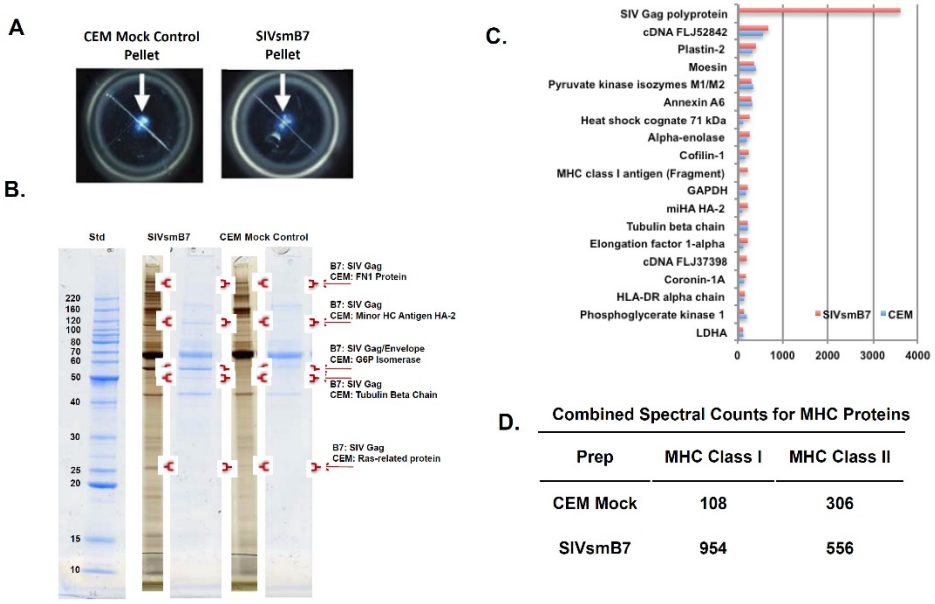

D. Combined Spectral Counts for MHC Proteins

Prep	MHC Class I	MHC Class II
CEM Mock	108	306
SIVsmB7	954	556

Figure S4. Proteomic analysis and comparison of SIVsmB7 and CEM control. (A) Picture of pellets after ultracentrifugation. Note the similarities in size and appearance of the pellets. (B) Silver staining of protein gels for CEM mock control and SIVsmB7 showed a high degree of similarity outside of five distinct bands in SIVsmB7 not found in CEM mock control. A colloidal stain was done to confirm the band differences. Once confirmed, those bands were excised for proteomic analysis. In each of these five bands, SIV gag polyprotein or envelope was identified. (C) Top 15 proteins for SIVsmB7 and CEM mock control organized by SIVsmB7 abundance. The list contains only 19 proteins, showing the high degree of protein composition similarity between the two. The only truly notable protein not found in CEM mock control is SIV gag polyprotein, which is the most abundant protein found in SIVsmB7. (D) Table showing the abundances of MHC protein fragments detected in SIVsmB7 or CEM Mock control. Individual spectral counts were grouped according to MHC Class I or Class II for clarity.

Method: SIVsmB7 is a virus-like particle (VLP) derived from a clone of a CEMx174 cell line infected with SIVsmH3 . Clone B7 cells have a single provirus integrated into their 20th chromosome. SIVsmB7 is noninfectious due to a 1.6 kbp deletion, including integrase, vif, vpr, and vpx genes [29]. To produce cell-free SIVsmB7 and CEM mock control, 200,000 cells/ml of Clone B7 and uninfected CEMx174 cells were cultured in RPMI 1640 (Mediatech, Inc.) supplemented with FBS. VLPs was purified on 20% (w/v) sucrose gradient by ultra-centrifugation. Figure 1B illustrates individual pellets from CEM mock control and SIVsmB7 after supernatants are removed. The pellet was resuspended in RPMI 1640 without supplementation. ELISA was done to measure P27 content. SIVsmB7 was diluted to a concentration of 500 μg P27 SIVsmB7 per 1 ml dose. CEMx174 dose was prepared using identical techniques.

Table S2. Proteomic Analysis of Individual Differential Bands from SIVsmB7 and CEM mock control samples

CEM Band Protein Name	Coverage	Spectral Count	SIVsmB7 Band Protein Name	Coverage	Spectral Count
Band 1			**Band 1**		
FN1 protein	14.80%	29	Gag Polyprotein	60%	71
Oleoyl-[acyl-carrier-protein] hydrolase	3.80%	6	Filamin-A	15%	27
Uncharacterized protein	2.20%	5	Desmoplakin	5.90%	17
Dermcidin isoform 2	18.20%	3	Junction plakoglobin	11.90%	7
Hornerin	4.50%	3	Desmoglein-1	9.10%	6
Type I keratin 16; K16	8.50%	2	Ubiquitin/40S ribosomal protein S27a	44.40%	6
Band 2			**Band 2**		
Minor Histocompatibility Antigen HA-2	23.00%	27	Gag Polyprotein	59.80%	130
Alpha Actin 4	27.60%	26	Minor histocompatibility HA-2	34.60%	51
Kinesin-like protein KIF23	17.20%	15	Kinesin-like protein KIF23	28.10%	26
Intercellular adhesion molecule 3	8.40%	7	Alpha-actinin	26.50%	26
cDNA FLJ56016, highly similar to C-1-tetrahydrofolate synthase, cytoplasmic	8.20%	9	Major vault protein	23.60%	18
Ubiquitin-like modifier-activating enzyme 1	8.10%	7	Putative helicase MOV-10	16.10%	17
Band 3			**Band 3**		
Glucose-6-phosphate isomerase	19.30%	14	Gag Polyprotein	75.70%	397
Pyruvate kinase isozymes M1/M2	30.10%	19	Tubulin beta chain	55.20%	26
cDNA FLJ61188, highly similar to Basigin	37.80%	13	cDNA FLJ37935 fis, clone CTONG2005290, highly similar to FASCIN	44.30%	23
Uncharaterized protein	31.10%	14	Coronin-1A	41.40%	18
cDNA FLJ37935 fis, clone CTONG2005290, highly similar to FASCIN	28.20%	14	cDNA FLJ61188, highly similar to Basigin	37.80%	9
Plastin-2	23.10%	13	cDNA FLJ32131 fis, highly similar to Tubulin alpha-ubiquitous chain	29.60%	6
Band 4			**Band 4**		
Tubulin beta chain	41.20%	29	Gag Polyprotein	44.40%	41
Alpha-enolase	39.60%	28	Alpha-Enolase	41.70%	39
Coronin-1A	25.60%	16	Tubulin beta chain	45.90%	35
Elongation factor 1-alpha	7.60%	5	Elongation factor 1-alpha	31.80%	26

APT synthast subunit beta, mitochondrial	15.10%	8	cDNA FLJ60299, highly similar to Rab GDP dissociation inhibitor beta	43.90%	23
Tubulin beta-2C chain	9.40%	5	Coronin-1A	20.00%	23
Band 5			**Band 5**		
Ras-related protein Rab-35	15.90%	4	Gag Polyprotein	37.70%	52
RAB11B protein	19.30%	4	cDNA FLJ75480, highly similar to Human lactoferrin	22.50%	15
60S ribosomal protein L18	13.80%	3	Ras-related protein Rab-35	24.80%	8
Uncharacterized protein	13.60%	3	Ras-related protein Rab-11A	34.70%	6
B-lymphocyte antigen CD20	12.80%	3	Elongation factor 1-alpha	9.70%	5
S-9 (Fragment)	19.00%	3	40S ribosomal protein S9	19.6%	4

Table S2. Results of individual band proteomic analysis for SIVsmB7 and CEM control. Top six proteins from each of the excised bands shown in figure 1 from CEM mock control [Left] and SIVsmB7 [Right]. As noted previously, SIV gag polyprotein was the dominant protein in each of those excised bands from SIVsmB7. The remaining proteins found in those bands were comparable to proteins identified from bands excised from CEM mock control taken from the same position in the CEM mock control lanes. Total coverage of the given protein is shown along with total spectral counts.